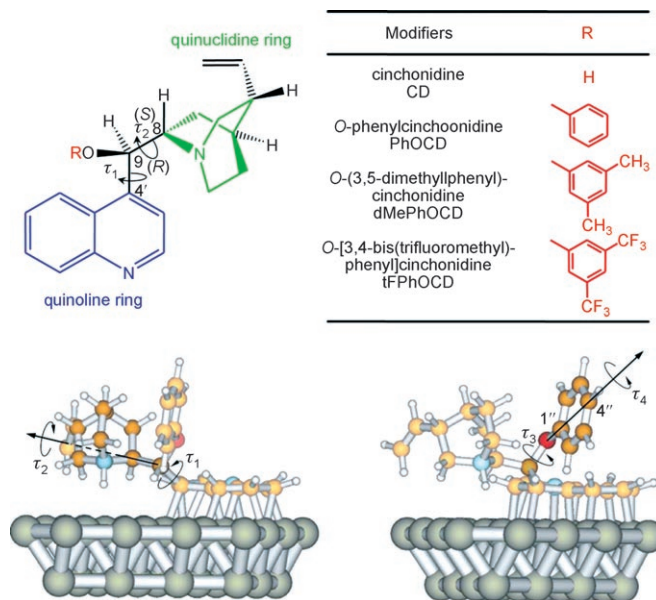


# Controlling the Sense of Enantioselection on Surfaces by Conformational Changes of Adsorbed Modifiers\*\*

Angelo Vargas, Davide Ferri, Norberto Bonalumi, Tamas Mallat, and Alfons Baiker\*

Heterogeneous catalysts are systems for which the chemical reactivity normally occurs at a solid–gas or solid–liquid interface. They are traditionally regarded as workhorses for large-scale chemical transformations (for example, oil cracking, ammonia synthesis, and olefin polymerization). Solid–gas interfaces have been thoroughly investigated, and an impressive understanding of their structure and reactivity has been reached.<sup>[1]</sup> In contrast, the understanding of solid–liquid interfaces, which are especially useful for the production of fine chemicals, lags behind, owing to their complexity and to the limited availability of suitable spectroscopic tools. This situation is particularly true for the chiral surfaces used in heterogeneous asymmetric catalysis.<sup>[2]</sup> While various analytical techniques relying on ultrahigh vacuum (UHV) conditions have provided fascinating insight on the structure of adsorbed chiral molecules,<sup>[3]</sup> transferring this information to the conditions governing liquid-phase reactions is not straightforward. Herein, we show that enantioselective heterogeneous catalysts derived from the platinum–cinchona-alkaloid system<sup>[2a–h]</sup> can generate chiral solid–liquid interfaces where subtle conformational changes of the carbon skeleton lead to inversion of the sense of enantioselection. This understanding opens interesting possibilities for the tailoring of solid–liquid interfaces.

The structural characterization of surface species presented in the following discussion is attained using attenuated total reflection infrared (ATR-IR) spectroscopy<sup>[4]</sup> in combination with density functional theory (DFT) calculations on metal clusters.<sup>[5]</sup> Cinchonidine (CD), *O*-phenylcinchonidine (PhOCD), and its ring-substituted derivatives *O*-[3,5-bis(trifluoromethyl)phenyl]cinchonidine (tFPhOCD) and *O*-(3,5-dimethylphenyl)cinchonidine (dMePhOCD) have been used as chiral surface modifiers of platinum in the hydrogenation of ethyl pyruvate and other activated ketones (Figure 1).<sup>[6]</sup> Cinchona alkaloids are anchored to the metal surface by the quinoline ring<sup>[7]</sup> and can interact with the prochiral ketone



**Figure 1.** Top: Chemical structures of the cinchona-alkaloid modifiers; the main submolecular moieties, the absolute configurations at C8 and C9, and the torsional angles  $\tau_1$  and  $\tau_2$  are indicated. Bottom: Two views of a stable conformer of PhOCD adsorbed on platinum; in addition to  $\tau_1$  and  $\tau_2$ , the two degrees of freedom associated with the phenyl ring, torsional angles  $\tau_3$  and  $\tau_4$ , are also indicated; Pt gray, C orange, H white, N blue, O red; the carbon atoms of the quinuclidine (left) and of the phenyl moieties (right) have been darkened.

through the tertiary amino group of the quinuclidine moiety.<sup>[2b–f,8]</sup>

The conformations of CD and PhOCD have been studied in vacuum, in solution, and upon adsorption on Pt(111).<sup>[9]</sup> Figure 1 shows two views of a stable conformer of PhOCD adsorbed on platinum, which indicate the remarkable conformational complexity of the system. Two rotational degrees of freedom (torsional angles  $\tau_1$  and  $\tau_2$ ) allow surface conformers characterized by different positions of the quinuclidine moiety;<sup>[5b]</sup> additionally, *O*-phenyl-substituted cinchonidines have two further rotational degrees of freedom (torsional angles  $\tau_3$  and  $\tau_4$ ) that allow conformers having different spatial arrangements of the phenyl ring. Note that the chiral site generated in proximity of the alkaloid is determined by the values of  $\tau_1$  and  $\tau_2$ , by the presence of the ether substituent, and by its position, which is set by  $\tau_3$  and  $\tau_4$ . The adsorption geometry and distribution of conformers on the surface can be investigated by assigning a spectroscopic feature to each molecular subunit. For this purpose, surface selection rules are applied, according to which only vibrational modes having at least a component of the dynamic

[\*] Dr. A. Vargas, Dr. D. Ferri, N. Bonalumi, Dr. T. Mallat, Prof. Dr. A. Baiker  
Institut für Chemie und Bioingenieurwissenschaften  
ETH Zürich  
Hönggerberg, HCI, 8093 Zürich (Switzerland)  
Fax: (+41) 44-632-1163  
E-mail: baiker@chem.ethz.ch  
Homepage: <http://www.baiker.ethz.ch>

[\*\*] The authors kindly acknowledge the Swiss National Science Foundation and the Foundation Claude and Giuliana for financial support, and the Swiss Centre for Scientific Computing (SCSC) in Manno for computing time.

Supporting information for this article is available on the WWW under <http://www.angewandte.org> or from the author.

dipole moment perpendicular to the surface can be detected.<sup>[10]</sup>

The transmission IR spectra of the cinchona-alkaloid modifiers in solution (Figure 2 f–i) are a combination of the spectra of CD and the corresponding substituted anisole, for which the assignment of the vibrational modes was reported elsewhere.<sup>[5c]</sup> Since adsorption is dominated by the interaction of the quinoline ring with platinum, the signals due to the

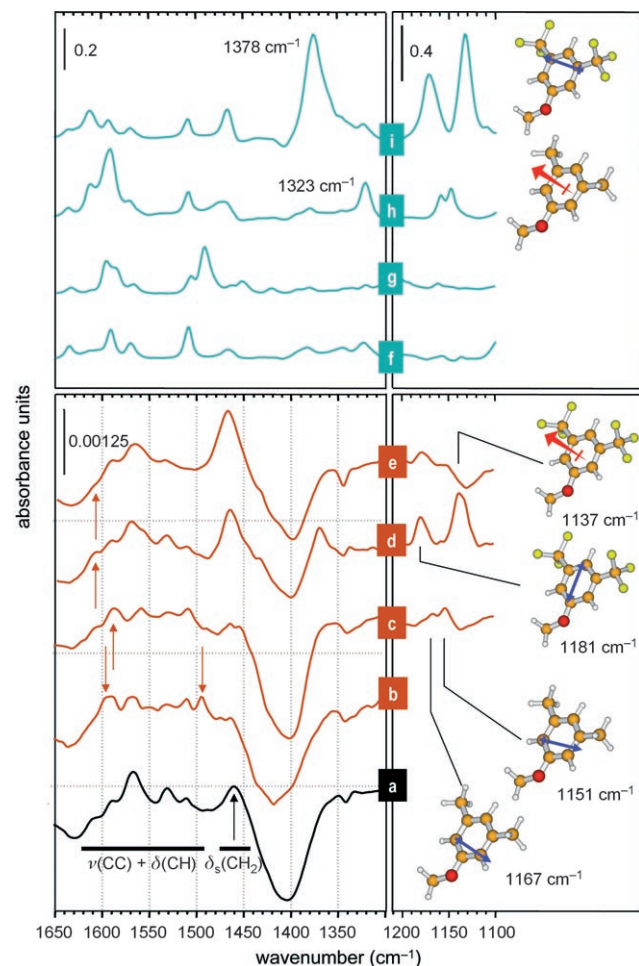


**Figure 2.** Bottom: ATR-IR spectra of the cinchona-alkaloid modifiers adsorbed on Pt/Al<sub>2</sub>O<sub>3</sub>: a) CD, b) PhOCD, c) dMePhOCD, and tFPhOCD d) before and e) after solvent flow. Conditions: 0.5 mm modifier, 293 K, CH<sub>2</sub>Cl<sub>2</sub> solvent, 1 h on stream (1 mL min<sup>-1</sup>). The signals between 1650 and 1500 cm<sup>-1</sup> are representative of three coexisting adsorbed species having different orientations of the quinoline ring with respect to the surface plane:<sup>[7b,c]</sup> flat species: 1570 cm<sup>-1</sup>; tilted species: 1590 and 1510 cm<sup>-1</sup>; and  $\alpha$ -quinolyl species: 1530 cm<sup>-1</sup>. The red arrows indicate the signals associated with the phenyl substituents. The black arrow indicates the envelope grouping the deformation modes of the quinuclidine moiety. The chemical structures illustrate the dynamic dipole moments of the normal modes (blue arrow: in the plane of the phenyl ring; red arrow: perpendicular to the plane) associated with the signals at 1167 and 1151 cm<sup>-1</sup> (c) for dMePhOCD, and at 1181 (d) and 1137 cm<sup>-1</sup> (e) for tFPhOCD. Top: Transmission IR spectra of the modifiers in solution: f) CD, g) PhOCD, h) dMePhOCD, and i) tFPhOCD. Conditions: 20 mm modifier, 293 K, CH<sub>2</sub>Cl<sub>2</sub> solvent, 1-mm pathlength. The chemical structures illustrate the dynamic dipole moments associated with the signals at 1323 cm<sup>-1</sup> (h) for dMePhOCD, and at 1378 cm<sup>-1</sup> (i) for tFPhOCD.

quinoline ring in the 1650–1500 cm<sup>-1</sup> region of the ATR-IR spectra (Figure 2 a–e) of all the modifiers are very similar, indicating a similar mode of interaction of the anchoring group with the surface.<sup>[6b,7b,c]</sup>

The orientation of the quinuclidine moiety can be qualitatively followed by studying the change in the intensity of the signal at 1460 cm<sup>-1</sup> (black arrow in Figure 2 a). This signal is composed of at least three deformation modes due to the CH<sub>2</sub> groups, which are very close in energy.<sup>[7b]</sup> In the ATR-IR spectra, this signal vanishes almost completely on passing from CD (Figure 2 a) to PhOCD (Figure 2 b), indicating a change in orientation: PhOCD has surface conformers characterized by a different orientation of the quinuclidine subunit with respect to that of CD.

Consider now the orientation of the phenyl ring of PhOCD. Its role is evidently critical, because its presence leads to the inversion of enantioselectivity, with respect to unsubstituted CD, in the enantioselective hydrogenation of ethyl pyruvate. Sampling the conformational space leads to several minimum-energy structures, of which the most meaningful for the present discussion are illustrated in Figure 3.

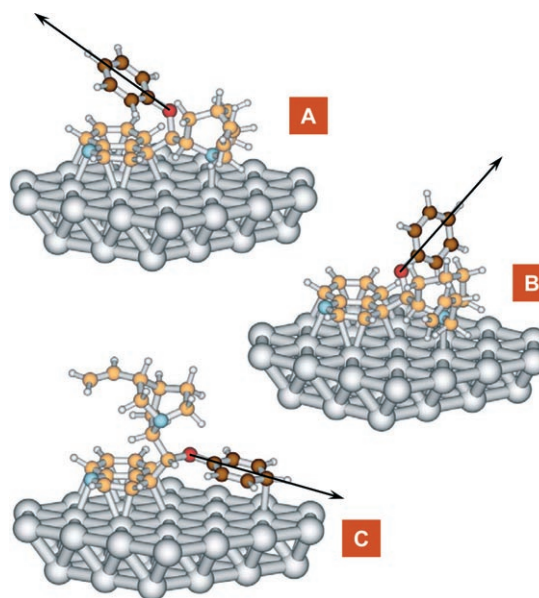


**Figure 3.** Three energetically similar conformations calculated for PhOCD adsorbed on a platinum surface. Note that in conformers **B** and **C** the phenyl ring is close to the metal surface and can interfere in the interaction with the substrate, while in conformer **A** the chiral site is similar to that of CD adsorbed on a platinum surface. The arrows indicate the C<sub>2</sub> axis of the phenyl ring. Pt gray, C orange, H white, N blue, O red; the carbon atoms of the phenyl moiety have been darkened.

DFT calculations identify three conformers which lie within an energy range of only 2 kcal mol<sup>-1</sup>. In conformer **A**, the phenyl ring is far from the metal surface (and above the quinoline ring); therefore, the chiral site of CD is reproduced. In contrast, in conformer **B**, the phenyl ring is approximately perpendicular to the surface and is located in the space beside the quinoline ring; the phenyl ring is, thus, close to the metal surface and interferes with the chiral site. In conformer **C**, the

phenyl ring lies approximately parallel to the surface, directly on the metal, and, therefore, also interferes with the chiral site. It should be emphasized that two of the three conformers, namely **B** and **C**, produce a chiral site that is different from that of **CD**. This finding is consistent with the results of catalysis studies, which have shown that the use of PhOCD as a modifier affords the *S* lactate, whereas the use of **CD** affords the *R* lactate in the enantioselective hydrogenation of ethyl pyruvate over modified platinum.<sup>[6a]</sup>

The presence of the calculated conformations on Pt can be confirmed by spectroscopic analysis. Conformers **A** and **B** are detected on the basis of the characteristic vibrational modes of the phenyl ring; these modes are visible in the spectra of PhOCD, dMePhOCD, and tFPhOCD on platinum (red arrows in Figure 2b–e), thus, revealing species which have the phenyl ring oriented nonparallel to the surface plane. Conformer **C** has to be detected on the basis of other signals because of the nearly flat orientation of the phenyl ring. According to the calculated structures in Figure 3, the orientation of the quinuclidine subunit in conformer **C** is different from that in the other conformers. This change in orientation is also evident from a comparison of the ATR-IR spectra of **CD** and PhOCD on platinum. Since the most stable surface conformer of **CD** was shown to be equivalent to conformer **A**,<sup>[5b]</sup> it follows from the differences in the intensities of the peak at  $1460\text{ cm}^{-1}$  in the two spectra that conformer **C** is also present for PhOCD on the platinum surface.<sup>[6b]</sup>

Furthermore, the determination of the orientation of the phenyl ring in conformers **A** and **B** is aided by the characteristic vibrational modes of the  $\text{CH}_3$  and  $\text{CF}_3$  groups in dMePhOCD and tFPhOCD, which are absent in **CD** and PhOCD. The orientation of the phenyl ring of dMePhOCD with respect to the surface plane and the molecular backbone can be assessed by analysis of the signals at  $1167$  and  $1151\text{ cm}^{-1}$ , which correspond mainly to  $\text{C}-\text{CH}_3$  stretches (Figure 2c).<sup>[5c]</sup> These vibrational modes, whose dipole moments are perpendicular to the  $\text{C}_2$  axis of the ring and lie in the plane of the ring, are detected in the spectrum of dMePhOCD on platinum. In contrast, the vibration at  $1323\text{ cm}^{-1}$  ( $\nu(\text{CC})_{\text{Ar}} + \nu(\text{CH}_3) + \delta(\text{CH})_{\text{Ar}}$ ),<sup>[5c]</sup> which exhibits a dynamic dipole moment perpendicular to the plane of the ring, is silent (Figure 2c), demonstrating that the plane of the phenyl ring in dMePhOCD is normal to the surface plane. Since the same conclusion has been reached for PhOCD<sup>[6b]</sup> these observations show that the chiral modifiers dMePhOCD and PhOCD, both of which afford the *S* lactate<sup>[6a]</sup> in the enantioselective hydrogenation of ethyl pyruvate on chirally modified platinum, have similar orientations of the phenyl ring (conformer **B** in Figure 3).

A different picture results from the analysis of the ATR-IR spectrum of the fluorinated derivative tFPhOCD. Although there is an indication that the phenyl ring in this case is also strongly tilted with respect to the surface plane, the reversed intensity ratio of the signals having  $\nu_{\text{as}}(\text{CF})$  character<sup>[5c]</sup> at  $1181$  and  $1137\text{ cm}^{-1}$  in the ATR-IR spectrum of tFPhOCD on platinum (Figure 2e) and in the transmission spectrum of tFPhOCD (Figure 2i) reveals that the ring is oriented with the  $\text{C}_2$  axis approximately normal to the plane

of the surface. This conformation is in contrast to those of dMePhOCD and PhOCD. The two vibrations have dynamic dipole moments along the  $\text{C}_2$  axis of the phenyl ring and perpendicular to the plane of the ring, respectively. Calculation of the surface conformations of tFPhOCD on platinum reveals that by far the most populated species is the one corresponding to conformer **A** in Figure 3. In fact, for tFPhOCD this conformation is approximately  $4\text{ kcal mol}^{-1}$  more stable than that corresponding to conformer **B** in Figure 3. The adsorption mode with the phenyl ring parallel to the metal (corresponding to conformer **C**) is not even feasible, owing to the low affinity of the phenyl ring to the surface because of the trifluoromethyl substituents.<sup>[5c]</sup> Hence, the phenyl ring of tFPhOCD is mainly positioned as in conformer **A** and, thus, causes no interference in the chiral space. As for **CD**, the use of tFPhOCD as a chiral modifier leads to the *R* lactate in the enantioselective hydrogenation of ethyl pyruvate on chirally modified platinum. Note that the spectrum in Figure 2d is representative of all the adsorbed species, whereas the spectrum recorded after rinsing the surface (Figure 2e) represents only the most strongly adsorbed species.

The preceding observations draw a simple but fascinating picture of the surface phenomena that lead to an inversion of the enantioselective properties of the chirally modified platinum catalyst. The position of the phenyl ring, which can be altered by substitution, induces a conformational change of the skeleton of the adsorbed modifier. As a consequence, catalysts modified by ether derivatives of **CD** bearing differently substituted phenyl rings yield enantiomers of opposite configuration. In simpler terms, the sense of enantioselection is correlated with the conformation of the carbon skeleton of the modifier adsorbed on the metal.

In a lock-and-key mechanism, the presence of some types of ether substituents on **CD**, such as the *O*-phenyl moiety, closes the chiral space to the *pro-R* face of the substrate and opens it to the *pro-S* face. In contrast, the presence of trifluoromethyl groups on the *O*-phenyl moiety causes a conformational rearrangement of the carbon backbone of the modifier, which reshapes the chiral space and restores the *pro-R* selectivity. The structural variation of the chiral site that arises from the conformational changes of the modifiers has a similar implication for the interaction models proposed in the literature.<sup>[2b–f,3d,8]</sup> These models assume that the substrate interacts with the tertiary nitrogen center of the quinuclidine moiety.

Therefore, transition-metal surfaces modified by flexible molecules, although less refined than biological catalysts, can operate with principles that are analogous to those of enzymes: an orbital-rich transition metal activates the incoming substrates toward a transformation, and the flexible (but controllable by low energy barriers) carbon skeleton of a modifier directs the substrate to adopt a specific orientation with respect to the surface, which is ready to deliver active hydrogen. This process of chiral recognition and reshaping sites on catalytic surfaces constitutes a template for the development of smart catalytic interfaces, which could lead to interesting possibilities in the synthesis of optically pure molecules.



## Experimental Section

Materials: CD (Fluka, 98%), PhOCD (Ubichem, > 99.8%), dMe-PhOCD (Ubichem, > 98.5%), tFPhOCD (Ubichem, > 99.8%), and CH<sub>2</sub>Cl<sub>2</sub> were used as received. N<sub>2</sub> (99.995 vol. %) and H<sub>2</sub> (99.999 vol. %) gases were supplied by PANGAS.

Film preparation: The Pt/Al<sub>2</sub>O<sub>3</sub> thin films used for ATR-IR spectroscopy were prepared on a 1-mm-thick trapezoidal germanium internal-reflection element (IRE; 52 × 20 × 1 mm<sup>3</sup>) by electron-beam vapor deposition, as described in detail elsewhere.<sup>[4b]</sup> First, a 50-nm film of Al<sub>2</sub>O<sub>3</sub> was deposited, and then a 1-nm film of platinum.

ATR-IR spectroscopy: ATR-IR spectra were recorded on a Bruker Optics IFS-66/S spectrometer equipped with a commercial ATR accessory (Optispec) and a mercury cadmium telluride (MCT) detector.<sup>[5c]</sup> Spectra were collected by co-adding 200 scans at a resolution of 4 cm<sup>-1</sup>. All measurements were performed at 293 K. N<sub>2</sub>-saturated CH<sub>2</sub>Cl<sub>2</sub> was circulated over the thin film at 1.0 mL min<sup>-1</sup> for approximately 45 min, using a peristaltic pump, until steady-state conditions were achieved. Before adsorption, the platinum film was treated with H<sub>2</sub>-saturated solvent for approximately 3 min. An H<sub>2</sub>-saturated solution of the modifier was then admitted to the cell for about 1 h. The film was subsequently rinsed with H<sub>2</sub>-saturated CH<sub>2</sub>Cl<sub>2</sub>.

DFT calculations: Calculations were performed using the ADF code<sup>[11]</sup> with a Becke–Perdew functional. The zero-order regular approximation (ZORA) and core potentials corrected for relativistic effects (Dirac) were used. A frozen-core approximation (4f for platinum and 1s for the Period 2 elements) was applied, and valence double-zeta (DZ) or double-zeta plus polarization (DZP) basis sets were used for platinum and the Period 2 elements, respectively. The geometry of the metal cluster was constrained; all other degrees of freedom were optimized.<sup>[5]</sup>

Received: November 24, 2006

Revised: January 15, 2007

Published online: April 19, 2007

**Keywords:** asymmetric heterogeneous catalysis · cinchona alkaloids · density functional calculations · IR spectroscopy · surface chemistry

- [1] P. L. J. Gunter, J. W. Niemantsverdriet, F. H. Ribeiro, G. A. Somorjai, *Catal. Rev. Sci. Eng.* **1997**, 39, 77–168.  
[2] a) Y. Orito, S. Imai, S. Niwa, G. Nguyen, *J. Synth. Org. Chem. Jpn.* **1979**, 37, 173–174; b) T. Bürgi, A. Baiker, *Acc. Chem. Res.* **2004**, 37, 909–917; c) M. Studer, H. U. Blaser, C. Exner, *Adv.*

- Synth. Catal.* **2003**, 345, 45–65; d) A. Baiker, *Catal. Today* **2005**, 100, 159–170; e) D. Y. Murzin, P. Maki-Arvela, E. Toukonniitty, T. Salmi, *Catal. Rev. Sci. Eng.* **2005**, 47, 175–256; f) M. Bartók, *Curr. Org. Chem.* **2006**, 10, 1533–1567; g) P. McMorn, G. J. Hutchings, *Chem. Soc. Rev.* **2004**, 33, 108–122; h) M. Heitbaum, F. Glorius, I. Escher, *Angew. Chem.* **2006**, 118, 4850–4881; *Angew. Chem. Int. Ed.* **2006**, 45, 4732–4762; i) T. Osawa, T. Harada, O. Takayasu, *Curr. Org. Chem.* **2006**, 10, 1513–1531.  
[3] a) J. M. Bonello, F. J. Williams, R. M. Lambert, *J. Am. Chem. Soc.* **2003**, 125, 2723–2729; b) K. H. Ernst, Y. Kuster, R. Fasel, C. F. McFadden, U. Ellerbeck, *Surf. Sci.* **2003**, 530, 195–202; c) R. Raval, *Nature* **2003**, 425, 463–464; d) S. Lavoie, G. Mahieu, P. H. McBreen, *Angew. Chem.* **2006**, 118, 7564–7567; *Angew. Chem. Int. Ed.* **2006**, 45, 7404–7407; e) T. E. Jones, C. J. Baddeley, *J. Mol. Catal. A* **2004**, 216, 223–231.  
[4] a) N. J. Harrick, *Internal Reflection Spectroscopy*, Wiley, New York, **1967**; b) D. Ferri, T. Bürgi, A. Baiker, *J. Phys. Chem. B* **2001**, 105, 3187–3195; c) T. Bürgi, A. Baiker, *Adv. Catal.* **2006**, 50, 227–283.  
[5] a) A. Vargas, T. Bürgi, A. Baiker, *J. Catal.* **2004**, 226, 69–82; b) A. Vargas, A. Baiker, *J. Catal.* **2006**, 239, 220–226; c) N. Bonalumi, A. Vargas, D. Ferri, A. Baiker, *J. Phys. Chem. B* **2006**, 110, 9956–9965.  
[6] a) S. Diezi, T. Mallat, A. Szabo, A. Baiker, *J. Catal.* **2004**, 228, 162–173; b) N. Bonalumi, A. Vargas, D. Ferri, T. Bürgi, T. Mallat, A. Baiker, *J. Am. Chem. Soc.* **2005**, 127, 8467–8477; c) A. Vargas, N. Bonalumi, D. Ferri, A. Baiker, *J. Phys. Chem. A* **2006**, 110, 1118–1127; d) D. Meier, T. Mallat, D. Ferri, A. Baiker, *J. Catal.* **2006**, 244, 260–263.  
[7] a) G. Bond, P. B. Wells, *J. Catal.* **1994**, 150, 329–334; b) D. Ferri, T. Bürgi, *J. Am. Chem. Soc.* **2001**, 123, 12074–12084; c) Z. Ma, I. Lee, J. Kubota, F. Zaera, *J. Mol. Catal. A* **2004**, 216, 199–207.  
[8] N. Bonalumi, T. Bürgi, A. Baiker, *J. Am. Chem. Soc.* **2003**, 125, 13342–13343.  
[9] a) G. D. H. Dijkstra, R. M. Kellogg, H. Wynberg, J. S. Svendsen, I. Marko, K. B. Sharpless, *J. Am. Chem. Soc.* **1989**, 111, 8069–8076; b) G. D. H. Dijkstra, R. M. Kellogg, H. Wynberg, *J. Org. Chem.* **1990**, 55, 6121–6131; c) M. Schürch, O. Schwalm, T. Mallat, J. Weber, A. Baiker, *J. Catal.* **1997**, 169, 275–286; d) T. Bürgi, A. Baiker, *J. Am. Chem. Soc.* **1998**, 120, 12920–12926; e) H. Caner, P. U. Biedermann, I. Agranat, *Chirality* **2003**, 15, 637–645.  
[10] R. G. Greenler, D. R. Snider, D. Witt, R. S. Sorbello, *Surf. Sci.* **1982**, 118, 415–428.  
[11] ADF, Version 2006.01, SCM, Vrije Universiteit, Amsterdam (The Netherlands), **2006**; <http://www.scm.com>; E. J. Baerends et al., see the Supporting Information.